Inorganic Chemistry
Article

Inorg. Chem. **2009**, *48*, 7491–7500 **7491**
DOI: 10.1021/ic900871g

Ligand Modifications for Tailoring the Binuclear Microenvironments in Schiff-Base Calixpyrrole Pacman Complexes†

Elham Askarizadeh,[‡,§] Aline M. J. Devoille,[‡] Davar M. Boghaei,[§] Alexandra M. Z. Slawin,[∥] and Jason. B. Love*[,‡]

[‡]*EaStCHEM School of Chemistry, University of Edinburgh, Joseph Black Building, The King's Buildings, West Mains Road, Edinburgh EH9 3JJ, U.K.,* [§]*Department of Chemistry, Sharif University of Technology, P.O. Box: 11155-3516, Tehran, Iran, and* [∥]*EaStCHEM School of Chemistry, University of St. Andrews, North Haugh, St. Andrews, Fife, KY16 9ST, U.K.* †*E. Askarizadeh and A. M. J. Devoille contributed equally to this work.*

Received May 6, 2009

The synthesis and structures of two new octadentate, Schiff-base calixpyrrole macrocycles are presented in which modifications at the *meso*-substituents (L^1) or the aryl spacer between the two pyrrole-imine donor compartments (L^2) are introduced. The outcomes of these changes are highlighted in the structures of binuclear Pacman complexes of these macrocycles, [$M_2(L^1)$] and [$M_2(L^2)$]. Both palladium and cobalt complexes of the fluorenyl-*meso*-substituted macrocycle H_4L^1 adopt rigid, but laterally twisted geometries with enclosed bimetallic microenvironments; a consequence of this spatial constraint is an *exo*-*exo*-bonding mode of pyridine in the dicobalt complex [$Co_2(py)_2(L^1)$]. In contrast, the use of an anthracenyl backbone between the two donor compartments (H_4L^2) generates a binuclear palladium complex in which the two PdN_4 environments are approximately cofacial and separated by 5.3 Å, so generating a bimetallic complex that is structurally very similar to binuclear compounds of cofacial diporphyrins.

Introduction

Strategies for the development of new catalysts suitable for multielectron redox reactions of small molecules that are fundamental to nascent energy technologies such as solar fuel and fuel cells often take inspiration from Nature where such reactions are catalyzed by metalloenzymes that contain precisely organized bi- or multimetallic reaction sites.[1] As such, the design of ligands that can promote the construction of bi- and multimetallic complexes that imitate or surpass enzymes as catalysts in these processes have both a long held fascination and increasing strategic significance.[2] In particular, numerous studies have been carried out on binuclear complexes of cofacial and Pacman diporphyrins and their corrole relatives as they have been shown to manage the multiple electron and proton inventory for a variety of redox reactions of small molecules including O_2, H_2O, N_2, and CO_2.[3,4] These binucleating ligands provide precisely controlled primary coordination environments for the metals, coupled with the ability to organize their intraspatial separation, which results in a well-defined bimetallic reaction microenvironment. However, the multistep synthetic routes to these compounds are challenging, and, as an alternative, we, and Sessler and co-workers, reported independently synthetic procedures to a series of straightforwardly prepared, binucleating Schiff-base calixpyrrole macrocycles (H_4L) that adopt "double-pillared" Pacman geometries on metal coordination.[5] In relation to the chemistry of small molecules, binuclear Fe(II) complexes of these macrocycles were shown to react with oxygen to form the oxo-bridged compounds [$Fe_2(\mu$-O)(L)],[6] while binuclear Co(II) complexes reduce and retain dioxygen within the macrocyclic cleft to form mixtures of the peroxo complex

*To whom correspondence should be addressed. E-mail: jason.love@ed.ac.uk. Fax: +44 131 6504743. Phone: +44 131 6504762.

(1) Collman, J. P.; Boulatov, R.; Sunderland, C. J.; Fu, L. *Chem. Rev.* **2004**, *104*, 561. Holm, R. H.; Kennepohl, P.; Solomon, E. I. *Chem. Rev.* **1996**, *96*, 2563. Barber, J. *Biochem. Soc. Trans.* **2006**, *34*, 619.

(2) Collman, J. P.; Fu, L.; Herrmann, P. C.; Zhang, X. *Science* **1997**, *275*, 949. Evans, D. J.; Pickett, C. J. *Chem. Soc. Rev.* **2003**, *32*, 268. Fryzuk, M. D.; Johnson, S. A. *Coord. Chem. Rev.* **2000**, *200*−*202*, 379. MacKay, B. A.; Fryzuk, M. D. *Chem. Rev.* **2004**, *104*, 385. Spencer, D. J. E.; Marr, A. C.; Schröder, M. *Coord. Chem. Rev.* **2001**, *219*−*221*, 1055. Du Bois, J.; Mizoguchi, T. J.; Lippard, S. J. *Coord. Chem. Rev.* **2000**, *200*−*202*, 443. Gavrilova, A. L.; Bosnich, B. *Chem. Rev.* **2004**, *104*, 349. Dempsey, J. L.; Esswein, A. J.; Manke, D. R.; Rosenthal, J.; Soper, J. D.; Nocera, D. G. *Inorg. Chem.* **2005**, *44*, 6879. Fukuzumi, S. *Chem. Lett.* **2008**, *37*, 808. Lewis, N. S.; Nocera, D. G. *Proc. Natl. Acad. Sci. U.S.A.* **2006**, *103*, 15729. Sala, X.; Romero, I.; Rodriguez, M.; Escriche, L.; Llobet, A. *Angew. Chem., Int. Ed.* **2009**, *48*, 2842.

(3) Collman, J. P.; Wagenknecht, P. S.; Hutchinson, J. E. *Angew. Chem., Int. Ed.* **1994**, *33*, 1537.

(4) Harvey, P. D.; Stern, C.; Gros, C. P.; Guilard, R. *Coord. Chem. Rev.* **2007**, *251*, 401. Rosenthal, J.; Nocera, D. G. *Prog. Inorg. Chem.* **2007**, *55*, 483. Rosenthal, J.; Nocera, D. G. *Acc. Chem. Res.* **2007**, *40*, 543.

(5) Love, J. B. *Chem. Commun.* **2009**, 3154.

(6) Veauthier, J. M.; Cho, W.-S.; Lynch, V. M.; Sessler, J. L. *Inorg. Chem.* **2004**, *43*, 1220.

Published on Web 07/02/2009

Chart 1. Ligand Design Strategies to Disfavor Single-Atom-Bridged Binuclear Complexes

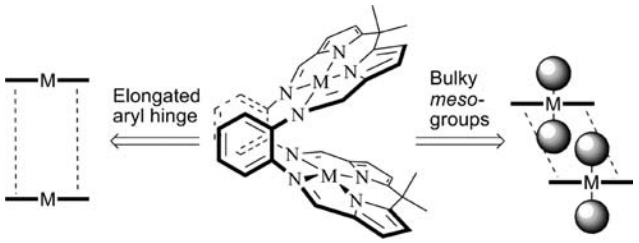

$[Co_2(\mu\text{-}O_2)(L)]$ and the superoxo cation $[Co_2(\mu\text{-}O_2)(L)]^+$.[7] Significantly, these latter cobalt Pacman complexes were shown to catalyze selectively the four-electron, four-proton reduction of dioxygen and furthermore, the mechanism of this reaction is thought to be similar to that for the cobalt diporphyrin analogues, in that the superoxo cation $[Co_2(O_2)(L)]^+$ is believed to be the catalytically relevant species.[8] Disappointingly, it was found that the rate of catalysis was very low with limited turnover, and it was reasoned that this was a consequence of the formation of the redox inactive peroxo complex and single-atom bridged species such as $[Co_2(\mu\text{-}OH)(L)]^+$.

To access more catalytically active binuclear complexes, it therefore appears important that the design of the bimetallic microenvironment should favor the formation of diatom-bridged intermediates over single-atom-bridged species. This rationale has been used to good effect in binuclear diporphyrin chemistry, in particular that related to oxo-atom transfer and oxygen evolution, where the use of bulky *meso*-mesityl substituents on the porphyrin rings causes the two metalloporphyrin units to "spring" apart and to disfavor the formation of inhibitory oxo- and hydroxo-bridges.[9,10] In our case, we reasoned that two complementary ligand design approaches could be used to overcome the problems associated with monoatom bridged complexes and to favor the formation of diatom-bridged complexes: (i) the incorporation of more sterically hindering *meso*-substitutents that would promote both a lateral twist and open the mouth of the cleft, and (ii) the use of elongated aryl hinges between the two N_4-donor compartments (Chart 1). These approaches make use of the intrinsic modularity of our ligand synthesis in that it is straightforward to modify the *meso*-substituents and aryl backbone as these components are derived from readily available ketones and aromatic diamines.

Herein we describe our initial research into two new macrocyclic ligand designs that use sterically rigid fluorenyl *meso*-substitutents or anthracenyl aryl backbones to generate new classes of binuclear macrocyclic Pacman complexes.

Experimental Section

General Procedures. The syntheses of diethyl-2,2′-dipyrromethane,[11] 2,2′-dipyrro-9-fluorene,[12] 1,8-diaminoanthracene,[13,14] $[PdCl_2(PhCN)_2]$,[15] and $[Co(THF)\{N(SiMe_3)_2\}_2]$[16] were carried out as described in the literature, with the final reduction step of 1,8-diaminoanthracene carried out in the dark to avoid decomposition. Pyrrole was distilled under reduced pressure prior to use. All other chemicals were used as purchased. The synthesis of the macrocycle H_4L^2 was carried out in the dark. The palladium complex $[Pd_2(L^2)]$ and the cobalt compounds $[Co_2(L^1)]$ and $[Co_2(py)_2(L^1)]$ were synthesized under nitrogen using Schlenk and glovebox techniques. Dry solvents (THF, CH_2Cl_2 and toluene) were purified by passage through Vacuum Atmospheres solvent drying towers, pyridine was distilled from potassium and stored over molecular sieves, $CDCl_3$ was stirred over activated alumina and trap-to-trap vacuum distilled, and d_8-THF and d_5-pyridine were dried over potassium, trap-to-trap vacuum distilled, and freeze−pump−thaw degassed three times. ^{1}H NMR spectra were recorded at 298 K on a Bruker ARX250, DPX360, DMX500, or AVA600 spectrometer at 250.13, 360.13, 500.13, and 599.81 MHz, respectively; $^{13}C\{^1H\}$ NMR spectra were recorded at 298 K on a Bruker ARX250, DPX360, or DMX500 at 62.90, 90.55, and 125.77 respectively. All ^{1}H NMR spectra were referenced internally to residual protio-solvent resonances. EPR spectra were recorded on a Bruker ER200D spectrometer operating at 9.14 GHz, and IR spectra were recorded on a JASCO FT/IR 460 Plus spectrometer in the range 4000−400 cm^{-1}. Electrospray mass spectra were recorded using a Thermo LCQ instrument and electron impact mass spectra using a Thermo MAT 900XP spectrometer. Elemental analyses were carried out by Mr. Stephen Boyer at the London Metropolitan University. UV−vis spectra were recorded in tetrahydrofuran (THF) or CH_2Cl_2 on a PerkinElmer Lambda 900 UV/vis/NIR Spectrophotometer.

Synthesis of 9,9-Bis(5-formylpyrrole-2-yl)fluorene, 2. Neat $POCl_3$ (0.69 mL, 7.41 mmol) was added dropwise to a stirred solution of 9,9-bis(pyrrole-2-yl)fluorene (1.00 g, 3.38 mmol) in *N*,*N*-dimethylformamide (DMF, 10 mL) at 0 °C, during which the color changed from red to red-brown. The mixture was stirred for 1 h at room temperature, after which the solution was cooled down to 0 °C and quenched by addition of H_2O (20 mL). Aqueous KOH (2M) was added slowly until the solution became strongly basic and colorless solids had precipitated. The solution was then boiled for 1 h, the solids collected by filtration, washed with water (3 × 50 mL), and dried under vacuum to yield 1.01 g, 85% of **2** as a colorless powder.

^{1}H NMR ($CDCl_3$, 360.13 MHz): δ_H 11.38 (br, N*H*, 2H), 8.90 (s, 2H, C*H*O), 7.92 (m, 2H, fluorenyl), 7.73 (m, 2H, fluorenyl), 7.35 (m, 4H, fluorenyl), 6.61 (d, 2H, pyrrole), 5.65 (d, 2H, pyrrole); $^{13}C\{^1H\}$ NMR ($CDCl_3$, 90.55 MHz): δ_C 178.6 (s, CHO), 147.4 (s, quaternary), 143.4 (s, quaternary), 139.8 (s, quaternary), 132.9 (s, quaternary), 128.5 (s, $CH_{fluorenyl}$), 128.4 (s, $CH_{fluorenyl}$), 126.1 (s, $CH_{fluorenyl}$), 121.6 (s, $CH_{pyrrole}$), 120.2 (s, $CH_{fluorenyl}$), 110.7 (s, $CH_{pyrrole}$), 56.1 (s, quaternary); IR (nujol): υ 3201 (N−H), 1656 (CH=O), 1634 (C=N) cm^{-1}; Analysis. Found: C, 78.17; H, 4.67; N, 8.15. $C_{23}H_{16}N_2O_2$ requires: C, 78.39; H, 4.58; N, 7.95%; UV−vis (CH_2Cl_2): λ_{max} 289 nm (ln ε 10.9 mol^{-1} L cm^{-1}).

(7) Givaja, G.; Volpe, M.; Edwards, M. A.; Blake, A. J.; Wilson, C.; Schröder, M.; Love, J. B. *Angew. Chem., Int. Ed.* **2007**, *46*, 584.
(8) Volpe, M.; Hartnett, H.; Leeland, J. W.; Wills, K.; Ogunshun, M.; Duncombe, B.; Wilson, C.; Blake, A. J.; McMaster, J.; Love, J. B. *Inorg. Chem.* **2009**, *48*, 5195.
(9) Hodgkiss, J. M.; Chang, C. J.; Pistorio, B. J.; Nocera, D. G. *Inorg. Chem.* **2003**, *42*, 8270. Rosenthal, J.; Luckett, T. D.; Hodgkiss, J. M.; Nocera, D. G. *J. Am. Chem. Soc.* **2006**, *128*, 6546. Rosenthal, J.; Pistorio, B. J.; Chng, L. L.; Nocera, D. G. *J. Org. Chem.* **2005**, *70*, 1885. Naruta, Y.; Sasayama, M.; Sasaki, T. *Angew. Chem., Int. Ed.* **1994**, *33*, 1839. Shimazaki, Y.; Nagano, T.; Takesue, H.; Ye, B.-H.; Tani, F.; Naruta, Y. *Angew. Chem., Int. Ed.* **2004**, *43*, 98.
(10) Naruta, Y.; Maruyama, K. *J. Am. Chem. Soc.* **1991**, *113*, 3595.
(11) Sobral, A. J. F. N.; Rebanda, N. G. C. L.; da Silva, M.; Lampreia, S. H.; Ramos Silva, M.; Beja, A. M.; Paixão, J. A.; Rocha Gonsalves, A. M. D. A. *Tetrahedron Lett.* **2003**, *44*, 3971.
(12) Song, M.-Y.; Na, H.-K.; Kim, E.-Y.; Lee, S.-J.; Kim, K. I.; Baek, E.-M.; Kim, H.-S.; An, D. K.; Lee, C.-H. *Tetrahedron Lett.* **2004**, *45*, 299.
(13) Gosztola, D.; Wang, B.; Wasielewski, M. R. *J. Photochem. Photobiol. A: Chem.* **1996**, *102*, 71.
(14) Sessler, J. L.; Mody, T. D.; Ford, D. A.; Lynch, V. M. *Angew. Chem., Int. Ed. Engl.* **1992**, *31*, 452.
(15) Lahaye, J.; Lagarde, R. *J. Catal.* **1970**, *60*, 270.
(16) Burger, H.; Wannagat, U. *Monatsh. Chem.* **1963**, *94*, 1007.

Synthesis of H_4L^1. A mixture of **2** (0.50 g, 1.42 mmol) and 4,5-dimethyl-2,3-phenylenediamine (0.19 g, 1.42 mmol) in methanol (20 mL) was warmed until some part of the solids were dissolved, giving a yellow suspension. Neat TFA (0.32 g, 2.8 mmol) was added dropwise, causing the entire residual solid to dissolve and yield a red solution. The mixture was stirred for 15 min, and then solid KOH was added slowly in portions causing the immediate precipitation of yellow solids. The solids were collected by filtration, washed with methanol (3 × 10 mL), and dried under vacuum to yield 0.60 g, 93% of H_4L^1 as a yellow powder. A sample of H_4L^1 was recrystallized from $CHCl_3$/hexane solution for elemental analysis, while single crystals suitable for X-ray diffraction were grown by Et_2O diffusion into a CH_2Cl_2 solution.

^{1}H NMR ($CDCl_3$, 360.13 MHz): δ_H 9.05 (br, N*H*, 4H), 8.20 (s, 4H, imino), 7.81 (d, 4H, J = 7.60 Hz, fluorenyl Ar*H*), 7.57 (d, 4H, J = 7.60 Hz, fluorenyl Ar*H*), 7.43 (t, J = 7.3 Hz, 4H, fluorenyl Ar*H*), 7.32 (t, J = 7.3 Hz, 4H, fluorenyl Ar*H*), 6.84 (s, 4H, phenyl Ar*H*), 6.54 (d, 4H, J = 3.3 Hz, pyrrole C*H*), 6.06 (d, 4H, J = 3.3 Hz, pyrrole C*H*), 2.20 (s, 12H, CH_3); ^{13}C{^{1}H} NMR ($CDCl_3$, 90.55 MHz): δ_C = 151.4 (s, imino), 148.4 (s, quaternary), 141.9 (s, quaternary), 140.9 (s, quaternary), 139.0 (s, quaternary), 135.2 (s, quaternary), 132.7 (s, quaternary), 129.6 (s, fluorenyl *C*H), 129.2 (s, fluorenyl *C*H), 126.6 (s, fluorenyl *C*H), 124.5 (s, phenyl *C*H), 121.6 (s, fluorenyl *C*H), 117.4 (s, pyrrole *C*H), 110.9 (s, pyrrole *C*H), 57.3 (s, quaternary), 20.2 (s, *C*H_3); IR (nujol): υ 3441 (N−H), 1616 (C=N), 1554 (C=C) cm^{-1}; UV−vis (CH_2Cl_2): λ_{max} 310 nm (ln ε 11.7 mol^{-1} L cm^{-1}); ESI-MS: m/z 905.4 (M+1$^+$, 76%); Analysis. Found: C, 68.43; H, 4.39; N, 10.04%. $C_{62}H_{48}N_8$.1.8 $CHCl_3$ requires: C, 68.45; H, 4.39; N, 10.01.

Synthesis of the Binuclear Palladium Complex $[Pd_2(L^1)]$. To a stirred solution of H_4L^1 (0.100 g, 0.11 mmol) in CH_2Cl_2 (15 mL) was added a solution of $[PdCl_2(PhCN)_2]$ (0.085 g, 0.22 mmol) in CH_2Cl_2 (10 mL). The resulting solution was stirred for 10 min at room temperature (RT) during which the solid dissolved and the color changed to light red. Then NEt_3 (0.2 mL) was added dropwise, and the resulting deep red solution was stirred for 16 h, reduced in volume, and the crude product precipitated by addition of hexane. The solid was extracted into toluene and filtered. The filtrate was evaporated, and the solids recrystallized from CH_2Cl_2/hexane at room temperature yielding 0.066 g, 54% of $[Pd_2(L^1)]$ as a brown/red powder. Single crystals suitable for X-ray diffraction were grown by slow evaporation of a Et_2O solution.

^{1}H NMR ($CDCl_3$, 360.13 MHz): δ_H 7.78 (d, 2H, fluorenyl Ar*H*), 7.49 (m, 2H, fluorenyl Ar*H*), 7.44 (m, 2H, fluorenyl Ar*H*), 7.41(m, 2H, fluorenyl Ar*H*), 7.39 (s, 4H, C*H*N), 7.31 (m, 2H, fluorenyl Ar*H*), 6.72 (m, 2H, fluorenyl Ar*H*), 6.68(s, 4H, phenyl, ArH), 6.60 (m, 2H, fluorenyl Ar*H*), 6.53 (d, 4H, J = 3.90 Hz, pyrrole C*H*), 6.01 (m, 2H, fluorenyl Ar*H*), 5.45 (d, 4H, J = 3.90 Hz, pyrrole C*H*), 2.10 (s, 12H, CH_3); ^{13}C{^{1}H} NMR ($CDCl_3$, 90.55 MHz): δ_C = 160.2 (s, imine), 149.7 (s, quaternary), 148.8 (s, quaternary), 148.2 (s, quaternary), 143.0 (s, quaternary), 141.8 (s, quaternary), 139.6 (s, quaternary), 139.1 (s, quaternary), 135.2 (s, quaternary) 129.9 (s, fluorenyl *C*H), 129.0 (s, fluorenyl *C*H), 128.6 (s, fluorenyl *C*H), 127.3 (s, fluorenyl *C*H), 126.9 (s, fluorenyl *C*H), 126.3 (s, fluorenyl *C*H), 125.1 (s, phenyl), 120.8 (s, fluorenyl *C*H), 120.1 (s, fluorenyl *C*H), 119.7 (s, pyrrole *C*H), 109.7 (s, pyrrole *C*H), 62.6 (s, quaternary), 20.3 (s, *C*H_3); IR (nujol): υ 1547 (C=N) cm^{-1}; UV−vis (CH_2Cl_2): λ_{max} 311 nm (ln ε 10.63 mol^{-1} L cm^{-1}); 415 (ln ε 10.06); ESI-MS: m/z 1115.4 (M$^+$+2, 6%); Analysis. Found: C, 66.53; H, 4.41; N, 9.94. $C_{62}H_{44}N_8Pd_2$ requires: C, 66.85; H, 3.98; N, 10.06%

Synthesis of $[Co_2(L^1)]$ and Its Pyridine Adduct $[Co_2(exo\text{-py})_2(L^1)]$. A solution of $[Co(THF)\{N(SiMe_3)_2\}_2]$ (1.82 g, 4.00 mmol) in THF (25 mL) was added dropwise to a suspension of H_4L^1 (1.81 g, 2.00 mmol) in THF (30 mL) at −78 °C. The mixture was stirred for 16 h at room temperature, after which it was evaporated to dryness under vacuum. The dark residues were extracted into warm toluene (ca. 50 °C, total 50 mL), filtered by cannula, and the filtrate evaporated to dryness under vacuum, yield 1.52 g, 75.0%. Dark-red crystals of $[Co_2(L^1)]$ were grown by hexane diffusion into toluene. Addition of pyridine to the same crystallization mixture generated dark red prisms of the bis (pyridine) adduct $[Co_2(exo\text{-py})_2(L^1)]$ that were suitable for X-ray crystallography.

^{1}H NMR ($CDCl_3$, 360.13 MHz): δ_H 74.6 (br.s, 4H), 39.5 (s, 4H), 1.44 (s, 2H), 1.13 (s, 2H), 0.60 (s, 2H), 0.20 (s, 2H), −2.40 (s, 2H), −3.16 (s, 2H), −11.2 (s, 12H), −24.5 (s, 2H), −32.2 (br.s, 4H), −43.4 (br.s, 2H), −51.2 (s, 4H); μ_{eff} ($CDCl_3$, 298 K) 3.24 μ_B; IR (nujol): υ 1551 (C=N) cm^{-1}; UV−vis (THF): λ_{max} 332 nm (ln ε 11.12 mol^{-1} L cm^{-1}), 257 (11.29), 221 (11.4); Analysis. Found: C, 73.16; H, 4.16; N, 10.93. $C_{62}H_{44}N_8Co_2$ requires: C, 73.14; H, 4.35; N, 10.98% $[Co_2(py)_2(L^1)]$ EPR (131 K, $CHCl_3$): g 2.217.

Synthesis of Dialdehyde 4. Neat $POCl_3$ (40.4 mL, 0.16 mol) was added dropwise to a stirred, cooled solution of **3** (40.0 g, 0.20 mol) in DMF (400 mL) at 0 °C. The cherry red reaction mixture was stirred at this temperature for 1 h and allowed to warm up to RT. The mixture was quenched with H_2O (400 mL) and 2 M KOH (1000 mL) which caused the precipitation of light pink solids. The suspension was warmed at 70 °C for 50 min, allowed to cool, and the solid filtered, washed with water until washings were neutral, and dried under vacuum to yield 40.0 g, 89% of **4** as a pale pink solid.

^{1}H NMR ($CDCl_3$, 250.13 MHz): δ_H 10.36 (s, 2H, N*H*), 9.05 (s, 2H, C*H*O, s), 6.76 (d, 2H, J = 4.0 Hz, pyrrole C*H*), 6.19 (d, 2H, J = 4.0 Hz, pyrrole C*H*), 1.98 (q, 4H, J = 7.4 Hz, CH_2), 0.65 (t, 6H, J = 7.4 Hz, CH_3); ^{13}C{^{1}H} NMR ($CDCl_3$, 62.90 MHz): δ_C 179.2 (s, C*H*O), 146.6 (s, quaternary), 132.6 (s, quaternary), 122.4 (s, *C*H), 111.1 (s, *C*H), (s, quaternary), 29.6 (s, *C*H_2), 8.7 (s, *C*H_3); Analysis. Found: C, 69.72; H, 7.04; N, 10.75. $C_{15}H_{18}N_2O$ requires: C, 69.74; H, 7.02; N, 10.84%

Synthesis of 1,8-Diaminoanthracene. 1,8-diaminoanthracene was prepared as reported in the literature from 1,8-dinitroquinone,[13,14] except the quinone reduction step was carried out in the dark and the diamine product was kept away from light at all times. The diamine was isolated as a bright yellow solid by filtration, washed with hexane and recrystallized from methanol at −80 °C to yield pale yellow needles in an overall 81% yield. The ^{1}H NMR data are identical to those reported previously.

^{1}H NMR (d_8-THF, 599.81 MHz): δ_H 8.65 (s, 1H, Ar*H*), 8.18 (s, 1H, Ar*H*), 7.26 (d, J = 8.4 Hz, 2H, Ar*H*), 7.16 (t, J = 7.8 Hz, 2H, Ar*H*), 6.58 (d, J = 7.1 Hz, 2H Ar*H*), 5.21 (s, 4H, N*H*); IR (nujol): υ 3427 (NH), 3373 (NH), 1583 (C=N), 1549 (C=C) cm^{-1}; UV−vis (THF): λ_{max} 356 nm (ln ε = 8.35 mol^{-1} L cm^{-1}), 375 (8.74), 419 (8.56); Analysis. Found: C, 80.64; H, 5.87; N, 13.38. $C_{14}H_{12}N_2$ requires: C, 80.74; H, 5.81; N, 13.45%

Synthesis of the Anthracenyl-Macrocycle H_4L^2. The reaction and work up were carried out in the dark. A suspension of diethyl-5,5′-diformyl-2,2′-dipyrromethane (2.46 g, 79.6 mmol) in MeOH (40 mL) was warmed until a clear solution was obtained and added to a suspension of 1,8-diaminoanthracene (2.00 g, 9.6 mmol) in MeOH (40 mL). Neat $(CF_3CO)_2O$ (1.60 mL, 11.5 mmol) was added dropwise at room temperature, the reaction mixture was stirred at ambient temperature for 30 min during which a bright orange precipitate formed. NEt_3 was added dropwise until the precipitate turned bright yellow. The mixture was stirred for a further 15 min, the solid filtered, washed with methanol, and dried under vacuum to yield 2.80 g, 68% of H_4L^2 as a yellow solid that was stored under N_2.

^{1}H NMR ($CDCl_3$, 250.13 MHz): δ_H 9.28 (s, 2H, N*H*), 9.22 (s, 2H, Ar*H*), 8.42 (s, 2H, Ar*H*), 8.37 (s, 4H, imino), 7.82 (d, 4H, J = 8.4 Hz, Ar*H*), 7.43 (t, 4H, J = 7,3 Hz, Ar*H*), 6.95 (d, 4H, J = 7.0 Hz, Ar*H*), 6.68 (d, 4H, J = 3.6 Hz, pyrrole C*H*), 6.23 (d, 4H, J = 3.7 Hz, pyrrole C*H*), 2.05 (q, 8H, J = 7.4 Hz, CH_2), 0.81 (t, 12H, J = 7.3 Hz, CH_3); ^{13}C{^{1}H} NMR ($CDCl_3$, 62.90 MHz): δ_C

150.6 (s, imine), 150.1 (s, quaternary), 140.83 (s, quaternary), 132.5 (s, quaternary), 130.6 (s, quaternary), 127.3 (s, quaternary), 126.2 (s, *C*H), 125.8 (s, *C*H), 125.2 (s, *C*H), 118.9 (s, *C*), 116.9 (s, *C*H), 112.8 (s, *C*H), 110.0 (s, *C*H), 45.5 (s, *meso-C*-pyrrole quaternary), 32.2 (s, CH_2), 9.1 (s, CH_3); IR (nujol): υ 3250 (N−H), 1613 (C═N), 1550 (C═C) cm^{-1}; UV−vis (THF): λ_{max} 322 nm (ln ε = 9.6 mol^{-1} L cm^{-1}), 370 (shoulder), 420 (shoulder); EI-MS: 860.5 (M^+, <1%), 831.5 (M^+ − 29, <1%, Et loss), 448.2 (M/2+18, 2%, water adduct), 430.2 (M/2, 100%), 401.1 (M/2 − 28, 86%, Et loss); ESI-MS: 897.27 (M+37, 28%), 861.74 (M, 40%), 431.72 (M/2 + 2, 40%); TLC: DCM/MeOH 97:3, Rf = 0.81, 0.62 (product); Analysis. Found: C, 80.84; H, 6.13; N, 12.94. $C_{58}H_{52}N_8$ requires: C, 80.90; H, 6.09; N, 13.01%

Synthesis of the Potassium Salt $[K_4(THF)_{2.65}(L^2)]$. To a stirred mixture of H_4L^2 (0.50 g, 0.58 mmol) and KH (0.12 g, 2.90 mmol) was added THF at −78 °C under nitrogen. The resulting solution was stirred for 1 h at −78 °C, allowed to reach room temperature, and stirred for a further 4 h. The deep red solution was decanted from the excess KH, and the solvent was removed under reduced pressure to yield 0.70 g, 74% of the potassium salt as a red solid.

^{1}H NMR (d_5-pyridine, 500.13 MHz): δ_H 10.02 (s, Ar*H*), 8.55 (s, Ar*H*), 8.41 and 8.34 (br.s, Ar*H*), 7.74 and 7.69 (br.d, J = 7.7 Hz, Ar*H*), 7.41 and 7.31 (br.t, J = 7.0 Hz, Ar*H*), 7.22 (m, Ar*H*+pyridine Ar*H*), 6.80 (m, pyrrole C*H*), 3.67 (m, THF), 3.49 and 3.14 (br, CH_2), 2.79 and 2.73 (br, CH_2), 1.63 (m, THF), 1.28 (br, CH_3); IR (nujol): υ 1583 (C═N), 1549 (C═C) cm^{-1}; Analysis. Found: C, 68.41; H, 5.66; N, 9.54. $C_{68.6}H_{62.2}N_8K_4O_{2.65}$ requires: C, 68.40; H, 5.79; N, 9.30%

Synthesis of the Binuclear Palladium Complex $[Pd_2(L^2)]$. A mixture of H_4L^2 (0.13 g, 0.015 mmol) and KH (0.03 g, 0.075 mmol) was combined in THF at −78 °C, allowed to warm to room temperature, and stirred for a further 4 h. The resulting mixture was transferred by filter cannula into a solution of $[PdCl_2(PhCN)_2]$ (0.15 g, 38.8 mmol) in THF shielded from light, and stirred for 20 days, after which the mixture was filtered, the solvent reduced under vacuum, and recrystallized at −78 °C to yield a yellow microcrystalline solid. Yield: 0.04 g, 23%

^{1}H NMR (d_8-THF, 500.13 MHz): δ_H 9.28 (s, 2H, Ar*H*), 7.80 (s, 2H, Ar*H*), 7.74 (s, 4H, imino), 7.34 (d, J = 8.8 Hz, 4H, Ar*H*), 6.93 (dd, J = 7.0 Hz, J = 1.0 Hz, 4H, Ar*H*), 6.84 (dd, J = 8.4 Hz, J = 7.0 Hz, 4H, Ar*H*), 6.81 (d, J = 4.0 Hz, 4H, pyrrole C*H*), 6.11 (d, J = 4.0 Hz, 4H, pyrrole C*H*), 2.15 (q, J = 7.2 Hz, 4H, CH_2), 1.89 (q, J = 7.3 Hz, 4H, CH_2), 0.51 (t, J = 7.2 Hz, 6H, CH_3), 0.27 (t, J = 7.3 Hz, 6H, CH_3); $^{13}C\{^1H\}$ NMR (d_8-THF, 125.77 MHz) δ_C 160.6 (s, imine), 145.0 (s, quaternary), 146.9 (s, quaternary), 138.2 (s, quaternary), 132.8 (s, quaternary), 127.9 (s, *C*H), 126.8 (s, quaternary), 126.6 (s, *C*H), 125.1 (s, *C*H), 120.7 (s, pyrrole *C*H), 119.4 (s, *C*H), 116.8 (s, *C*H), 109.0 (s, pyrrole *C*H), 40.0 (s, CH_2), 36.6 (s, CH_2), 11.2 (s, CH_3), 10.4 (s, CH_3). The poor solubility of the compound prevented the assignment of the quaternary *meso*-carbon; IR (nujol): υ 1616 (w), 1570 (*C*═*N*), 1552 (*C*═*C*) cm^{-1}; UV−vis (THF): λ_{max} 314 nm (ln ε = 11.0 mol^{-1} L cm^{-1}), 411 (10.1), 433 (9.9); ESI-MS: 1095.21 (M+2+23, 44%, Na^+ adduct), 1094.23 (M+1+23, 46%, Na^+ adduct), 1093.16 (M+23, 64%, Na^+ adduct), 1092.19 (M-1+23, 57%, Na^+ adduct), 1091.2 (M-2 + 23, 63%, Na^+ adduct), 1090.2 (M-3 + 23, 52%, Na^+ adduct). 1072.3 (M+2, 29%), 1071.2 (M+1, 34%), 1070.2 (M, 34%), 1069.2 (M-1, 31%), 1068.2 (M-2, 31%), 1067.1 (M-3, 24%); Analysis. Found: C, 64.89; H, 4.86; N, 9.93. $C_{58}H_{48}N_8Pd_2$ requires: C, 65.11; H, 4.52; N, 10.47%.

Alternative Synthesis of $[Pd_2(L^2)]$. A solution of $[PdCl_2(PhCN)_2]$ (0.02 g, 0.06 mmol) in THF (1 mL) was added to a solution of H_4L^2 (0.05 g, 0.06 mmol) in THF (4 mL) and stirred at room temperature for 30 min. A few drops of NEt_3 were added, and the reaction mixture was stirred for a further 3 days at room temperature. The mixture was treated with toluene and solvent was removed under reduced pressure. The crude mixture was analyzed by ^{1}H NMR spectroscopy in $CDCl_3$ from which crystals suitable for X-ray diffraction deposited.

^{1}H NMR ($CDCl_3$, 250.13 MHz): δ_H 9.08 (s, 2H, Ar*H*), 8.27 (s, 2H, Ar*H*), 8.22 (s, 4H, Ar*H*), 7.67 (d, 4H, J = 8.70 Hz, Ar*H*), 7.27 (m, 4H, Ar*H*), 6.78 (m, 4H, Ar*H*), 6.58 (d, 4H, J = 3.72 Hz, pyrrolic C*H*), 6.10 (d, 4H, J = 3.73 Hz, pyrrolic C*H*), 1.54 (m, 4H CH_3CH_2).

Crystallographic Details. X-ray diffraction data from single crystals of H_4L^1 and $[Co_2(exo\text{-}py)_2(L^1)]$ were collected at 93.15 K using graphite monochromated Mo Kα radiation (λ = 0.71073 Å) on a Rigaku MM007 diffractometer equipped with a high brilliance Saturn 70 CCD detector. The data for $[Pd_2(L^1)]$, $[Co_2(L^1)]$, H_4L^2, and $[Pd_2(L^2)]$ were collected at 150 K on a Bruker SMART APEX diffractometer equipped with a CCD detector. Details of the individual data collections and refinements are given in Table 1. All structures were solved by direct methods and refined using full-matrix least-squares refinement on $|F|^2$ using SHELXL-97. All non-hydrogen atoms were refined with anisotropic displacement parameters while hydrogen atoms were placed at calculated positions and included as part of a riding model. The X-ray data for H_4L^1 was collected on a weakly diffracting crystal although the macrocycle is well-defined in the model. The solvent of crystallization in H_4L^2 was diffuse and disordered and could not be modeled accurately so the corresponding electron density was accounted for using the SQUEEZE routine of PLATON. Three voids were found which was equated to 2 molecules of CH_2Cl_2 and 6.5 molecules of MeOH in the unit cell. Similarly, the Et_2O solvent of crystallization in the structure of $[Pd_2(L^1)]$ could not be modeled accurately, and two voids were found using the SQUEEZE routine of PLATON that equate to 2.5 molecules of Et_2O per asymmetric unit. The high residual electron densities seen in the structure of $[Pd_2(L^1)]$ are located close to the Pd centers and are not due to unidentified solvent atoms. The data for $[Co_2(L^1)]$ were weak and resulted in a model with high residual electron density. The data for $[Co_2(py)_2(L^1)]$ were also weak, and 0.25 molecules of PhMe per asymmetric unit were modeled isotropically, while the remaining unidentified solvent of crystallization was accounted for using the SQUEEZE routine of PLATON and modeled as 3.5 molecules of PhMe in the unit cell. In the asymmetric unit of the structure of $[Pd_2(L^2)]$, one molecule of chloroform was disordered about an inversion center and what appeared to be one molecule of disordered triethylamine was modeled using the SQUEEZE routine of PLATON. Two distinct voids were found with electron density appropriate for one molecule of NEt_3 per asymmetric unit.

Results and Discussion

Synthesis and Structures of H_4L^1 and H_4L^2. Although the synthesis of dipyrromethanes from bulky ketones can be problematic, we reported recently that the acid-catalyzed condensation reaction between pyrrole and 3,3,5,5-tetramethylcyclohexanone formed the corresponding dipyrromethane;[17,18] furthermore, we found that it was possible to use this dipyrromethane as a precursor to the [2+2] Schiff-base pyrrole macrocycle. As an alternative, we reasoned that planar aromatic substituents would provide excellent steric hindrance that would promote a laterally twisted conformation in $[M_2(L)]$ structures, and noted that the *meso*-fluorenyl-dipyrromethane **1**

(17) Givaja, G.; Volpe, M.; Leeland, J. W.; Edwards, M. A.; Young, T. K.; Darby, S. B.; Reid, S. D.; Blake, A. J.; Wilson, C.; Wolowska, J.; McInnes, E. J. L.; Schröder, M.; Love, J. B. *Chem.—Eur. J.* **2007**, *13*, 3707.
(18) Swartz, D. L. II; Odom, A. L. *Dalton Trans.* **2008**, 4254.

Table 1. Crystal Data[a]

	$H_4L^1(CH_2Cl_2)_2$	$H_4L^2(CH_2Cl_2)(CH_3OH)_{3.25}$	$[Pd_2(L^1)](Et_2O)_{2.5}$	$[Co_2(L^1)](PhMe)_2$	$[Co_2(py)_2(L^1)](PhMe)_{1.125}$	$[Pd_2(L^2)](NEt_3)(CHCl_3)$
cell setting, space group	monoclinic, $P2_1/n$	triclinic, $P\bar{1}$	monoclinic, $P2_1/n$	monoclinic, $P2_1/n$	monoclinic, $P2_1/a$	monoclinic, $C2/c$
a, b, c (Å)	15.839(5), 13.681(4), 24.855(7)	13.6736(3), 15.7991(4), 16.2295(4)	16.1288(9), 15.6072(9), 24.1738(14)	26.1784(8), 15.5384(5), 30.3722(10)	10.112(3), 47.309(13), 13.901(4)	12.453(3), 24.437(6), 19.712(5)
α, β, γ (deg)	90, 95.001(6), 90	71.0490(10), 87.508(2), 72.9140(10)	90, 95.951(3), 90	90, 107.883(2), 90	90, 94.66(7), 90	90, 103.965(5), 90
V (Å^3)	5366(3)	3164.44(13)	6052.4(6)	11757.6(6)	6628(3)	5822(2)
Z	4	2	4	8	4	4
D_x (Mg m^{-3})	1.331	1.101	1.420	1.359	1.305	1.472
Crystal size (mm)	0.05×0.05×0.03	0.53×0.33×0.24	0.50×0.29×0.18	1.2×0.1×0.1	0.1×0.1×0.1	0.20×0.10×0.10
absorption correction	none	multiscan	multiscan	multiscan	multiscan	multiscan
T_{min}		0.494	0.618	0.551	0.899	0.701
T_{max}		0.746	0.746	0.745	1.000	1.000
no. of measured, independent and observed reflections	52341, 9789, 5426	43492, 17436, 9246	80872, 17650, 14732	89934, 24105, 18468	39232, 11822, 7792	23819, 5241, 4687
θ_{max} (deg)	25.3	30.5	30.6	26.4	25.3	25.5
$R[F^2 > 2\sigma(F^2)]$, $wR(F^2)$, S	0.127, 0.330, 1.12	0.086, 0.159, 1.07	0.130, 0.303, 1.12	0.175, 0.308, 1.33	0.095, 0.295, 1.05	0.071, 0.200, 1.09
no. of parameters	689	598	650	1491	778	348
H-atom treatment	riding	riding	riding	riding	riding	riding
$\Delta\rho_{max}$, $\Delta\rho_{min}$ (e Å^{-3})	1.09, −0.48	0.63, −0.32	5.89, −3.43	1.24, −1.16	1.27, −0.60	0.78, −0.98
CSD numbers[a]	730679	730680	730681	730682	730683	730684

[a] CCDC 730679−730684 contain the supplementary crystallographic data for this paper. These data can be obtained free of charge from the Cambridge Crystallographic Data Centre via www.ccdc.cam.ac.uk/data_request/cif.

Scheme 1. Synthesis of the Fluorenyl and Anthracenyl Schiff-Base Calixpyrroles H_4L^1 and H_4L^2 and Their Binuclear Pd and Co Complexes

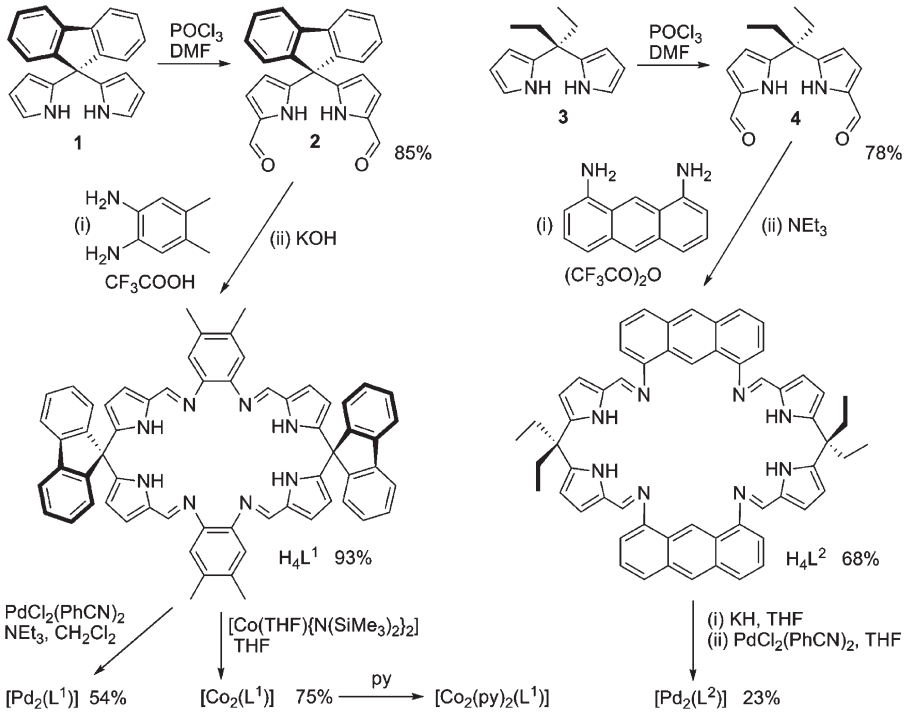

had been used in the synthesis of calixpyrroles and in conformational studies of calix[4]phyrins.[12,19] As such, **1** was prepared as described in the literature by reacting fluorenone with pyrrole under acidic conditions,[12] and was formylated in the 5, 5′-positions using a $POCl_3$/DMF Vilsmeier−Haack procedure described by us previously (Scheme 1);[20] the resulting dialdehyde **2** displayed a resonance at 8.90 ppm in the ^{1}H NMR spectrum that is characteristic of the C(H)═O group. Using the method

(19) Turner, B.; Botoshansky, M.; Eichen, Y. *Angew. Chem., Int. Ed.* **1998**, *37*, 2475. Dolensky, B.; Kroulik, J.; Kral, V.; Sessler, J. L.; Dvorakova, H.; Bour, P.; Bernatkova, M.; Bucher, C.; Lynch, V. *J. Am. Chem. Soc.* **2004**, *126*, 13714.

(20) Love, J. B.; Blake, A. J.; Wilson, C.; Reid, S. D.; Novak, A.; Hitchcock, P. B. *Chem. Commun.* **2003**, 1682.

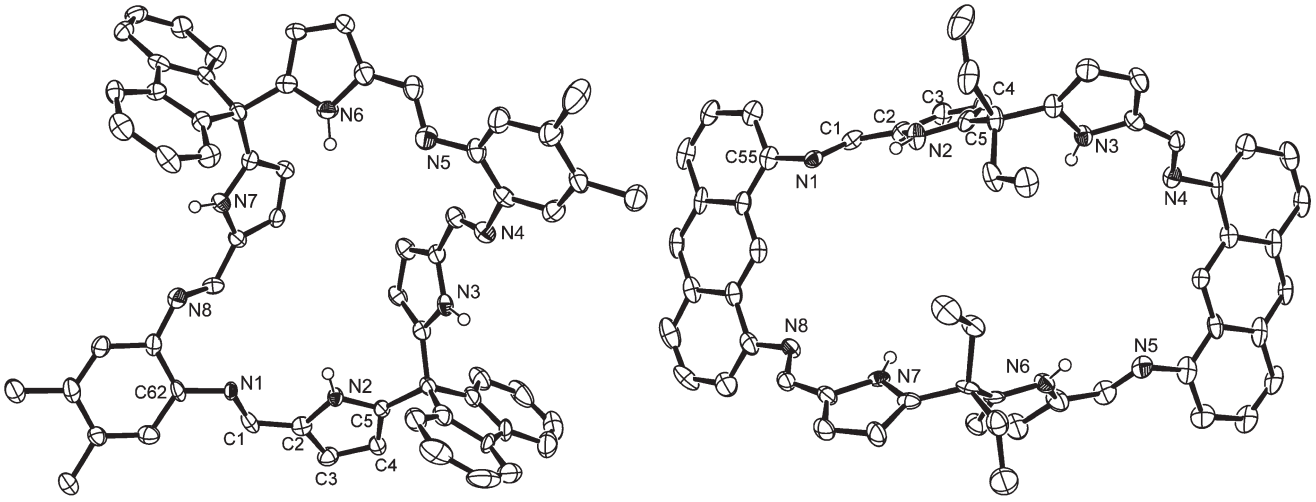

Figure 1. X-ray crystal structures of $H_4L^1(CH_2Cl_2)_2$ (left) and $H_4L^2(CH_2Cl_2)(MeOH)_{3.25}$ (right). For clarity, all hydrogen atoms, except those bound to the pyrrolic nitrogens, and solvent of crystallization are omitted (displacement ellipsoids are drawn at 50% probability).

described by us,[21] and independently by Sessler and coworkers,[22] we found that the reaction between **2** and 3,4-Me_2-1,2-diaminobenzene in the presence of CF_3CO_2H in methanol resulted in the sole formation of the acid salt of the [2 + 2] macrocycle $H_4L^1(CF_3CO_2H)_n$ as an orange solid. Neutralization of this salt with KOH in MeOH caused the rapid precipitation of the macrocycle H_4L^1 as an analytically pure yellow solid in high yield.

The ^{1}H NMR spectrum of H_4L^1 displays resonances consistent with the formation of a symmetric Schiff-base calixpyrrole, with the resonance at 8.20 ppm characteristic of the C(H)═N imine proton. The electrospray mass spectrum showed a parent ion at m/z 905 that supports the formation of the [2+2] condensation product, and there was no indication of any other lower or higher order condensation products.

To synthesize a macrocycle in which the two N_4-donor compartments were more separated vertically, we chose to use 1,8-anthracenediamine as the hinge component as this would be liable to act as a rigid double-pillar in the resulting $[M_2(L)]$ complexes. While not reported in the literature, we found that 1,8-diaminoanthracene was light sensitive and decomposed rapidly in solution to an intractable dark solid, presumably as a result of radical polymerization. As such, the synthesis and recrystallization of this diamine was carried out in the dark to afford analytically pure, pale yellow crystals of the diamine from methanol in good yield. Furthermore, to enhance the solubility of the macrocyclic product in nonpolar solvents, the new dialdehyde **4** was generated in good yield by the Vilsmeier−Haack formylation of *meso*-diethyldipyrromethane **3**. In a similar manner to above, dialdehyde **4** reacts with 1,8-diaminoanthracene in MeOH in the presence of acid (in this case generated from trifluoroacetic anhydride) to form the [2+2] macrocyclic orange acid salt $H_4L^2(TFA)_n$, that, upon neutralization with NEt_3, yields H_4L^2 as an analytically pure bright yellow solid. Because of the potential reversibility of the imine bond formation in a wet environment, the synthesis of H_4L^2 was carried out in the dark to prevent the formation of the diaminoanthracene and subsequent light-induced decomposition. However, once dry, the ligand can be stored indefinitely under a dry nitrogen atmosphere in the presence of light. The ^{1}H NMR spectrum of H_4L^2 supports the formation of a single, symmetric macrocycle and displays a single resonance at 8.34 ppm characteristic of imine bond formation and a broad resonance at 9.28 ppm integrating for the four pyrrolic N−H groups. In the electrospray mass spectrum of H_4L^2, a parent ion was seen at m/z 861 and also a doubly charged base peak at m/z 430; these data support the sole formation of the [2 + 2] macrocycle, and not any lower or higher order macrocyclic products.

X-ray quality crystals of H_4L^1 and H_4L^2 were grown by diffusion of Et_2O into a solution of CH_2Cl_2, and MeOH into CH_2Cl_2, respectively, and the crystal structures determined (Figure 1). Crystal data are displayed in Table 1, and selected bond lengths and angles are detailed in Table 2.

In the solid state, the fluorenyl-macrocycle H_4L^1 adopts a shallow bowl-shaped structure which hinges at the *meso*-carbons, with the fluorenyl groups essentially orthogonal to the macrocyclic plane. The pyrrole-imine units alternate *exo*- and *endo*- within the macrocyclic framework and are involved in hydrogen-bonding interactions with the CH_2Cl_2 solvent of crystallization (e.g., N2···Cl 3.783 Å) and $\pi-\pi$ stacking interactions with neighboring molecules. Similarly, the anthracenyl macrocycle adopts a wedge shape that is also hinged at the *meso*-carbons in the solid state with ill-defined solvent molecules present within the cleft; both of these structures are consistent with the propensity of this class of ligand to act as both hydrogen bond donor and acceptors.[5,23] All the bond distances and angles in H_4L^2 are similar to those observed in related ligands,[17,21] although the bond angle at the imine nitrogen in H_4L^2 is slightly more contracted than in previous structures and in H_4L^1 (average C1−N1−C_{aryl} 116.1° cf. 120.8°).

(21) Givaja, G.; Blake, A. J.; Wilson, C.; Schröder, M.; Love, J. B. *Chem. Commun.* **2003**, 2508.
(22) Sessler, J. L.; Cho, W.-S.; Dudek, S. P.; Hicks, L.; Lynch, V. M.; Huggins, M. T. *J. Porphyrins Phthalocyanines* **2003**, *7*, 97.
(23) Sessler, J. L.; Cambiolo, S.; Gale, P. A. *Coord. Chem. Rev.* **2003**, *240*, 17.

Table 2. Selected bond lengths [Å] and angles [deg] for: $H_4L^1(CH_2Cl_2)_2$; $H_4L^2(CH_2Cl_2)(MeOH)_{3.25}$; $[Pd_2(L^1)](Et_2O)_{2.5}$; $[Co_2(L^1)](PhMe)_2$; $[Co_2(py)_2(L^1)](PhMe)_{1.125}$; and $[Pd_2(L^2)](NEt_3)(CDCl_3)$

	$H_4L^1(CH_2Cl_2)_2$	$H_4L^2(CH_2Cl_2)$ $(CH_3OH)_{3.25}$	$[Pd_2(L^1)](Et_2O)_{2.5}$	$[Co_2(L^1)](PhMe)_2$	$[Co_2(py)_2(L^1)]$ $(PhMe)_{1.125}$	$[Pd_2(L^2)](NEt_3)$ $(CDCl_3)$
N1−C1	1.280(8)	1.270(6)	1.322(11)	1.317(12)	1.290(7)	1.325(8)
N1−C26A						1.416(7)
N1−C55		1.422(6)				
N1−C62	1.416(7)		1.405(10)	1.429(11)	1.448(7)	
C1−C2	1.427(8)	1.427(7)	1.427(8)	1.394(13)	1.433(8)	1.399(10)
C2−C3	1.392(8)	1.380(6)	1.392(8)	1.377(14)	1.392(7)	1.398(9)
N2−C2	1.376(7)	1.380(5)	1.356(10)	1.389(12)	1.389(7)	1.373(7)
N2−C5	1.362(7)	1.361(6)	1.338(10)	1.355(12)	1.331(6)	1.361(8)
C3−C4	1.413(8)	1.406(7)	1.382(14)	1.389(14)	1.381(8)	1.373(10)
C4−C5	1.377(8)	1.370(6)	1.396(13)	1.397(13)	1.399(7)	1.405(8)
M1−N1			2.043(7)	1.945(7)	1.974(4)	2.082(5)
M1−N2			1.933(7)	1.866(7)	1.871(4)	1.933(5)
M1−N3			1.931(7)	1.970(8)	1.867(4)	1.927(5)
M1−N4			2.076(8)	1.856(7)	1.984(4)	2.068(4)
M1···M2			3.72	3.64	4.12	5.38
C1−N1−C26A						119.3(5)
C1−N1−C55		115.9(4)				
C1−N1−C62	119.7(5)		119.7(5)	115.8(8)	117.9(4)	
N1−M1−N2			79.7(3)	82.7(3)	81.60(19)	80.4(2)
N2−M1−N3			88.8(3)	87.7(3)	87.30(19)	87.7(2)
N3−M1−N4			80.3(3)	83.2(3)	83.01(19)	81.03(18)
N4−M1−N1			110.9(3)	105.43(18)	105.43(18)	110.7(2)

Synthesis and Structure of $[Pd_2(L^1)]$. The reaction between H_4L^1 and $[PdCl_2(PhCN)_2]$ in the presence of NEt_3 resulted in the formation of the dark red, binuclear palladium complex $[Pd_2(L^1)]$ in good yield (Scheme 1). The presence of eight fluorenyl hydrogens in the ^1H NMR spectrum of $[Pd_2(L^1)]$ suggests that a C_2-symmetric Pacman geometry is present in solution with one-half of the fluorenyl group *endo*- to the molecular cleft, and the other half *exo*. Furthermore, the lack of NH resonances, and a decrease in the C=N vibration from 1616 in the IR spectrum of H_4L^1 to 1547 cm^{-1} in $[Pd_2(L^1)]$ are consistent with the coordination of the metal. This structure is retained in the solid state, as shown in the X-ray crystal structure of $[Pd_2(L^1)]$ (Figure 2); crystal data are shown in Table 1, and selected bond lengths and angles in Table 2.

In $[Pd_2(L^1)]$, the two metals Pd1 and Pd2 sit in approximately square-planar N_4-pyrrole-imine donor environments, in which the sum of the angles at Pd1 is 359.8° and at Pd2 is 359.9°, with out-of-plane distances 0.086 and 0.073 Å, respectively. As seen by us previously in similar complexes,[5] the presence of the aryl groups between the two donor compartments results in a Pacman geometric arrangement. As such, the aryl groups act as hinges and π-stack with a shortest interatomic distance of 3.56 Å, and converge toward the metals with an interplanar angle of 11.2°. The *pseudo*-porphyrinic cavities are not entirely planar because of the flexibility of the N_4-donor set at the sp^3-hybridized *meso*-carbons which results in dihedral angles between the pyrrole-imine planes of 20.6° at Pd1 and 15.5° at Pd2. Gross structural parameters including the M···M separation, lateral twist, and vertical bite angles for $[Pd_2(L^1)]$ can be compared to those of similar complexes described by us previously, in the particular with the binuclear palladium complexes $[Pd_2(L^{Me8})]$ and $[Pd_2(L^{Ph4Me4})]$ which differ only in their *meso*-substitution pattern, that is, $[Pd_2(L^{Me8})]$ has methyl *meso*-substituents while those in $[Pd_2(L^{Ph4Me4})]$ are phenyl (Table 3).[17] While crystal packing does appear to have an effect on

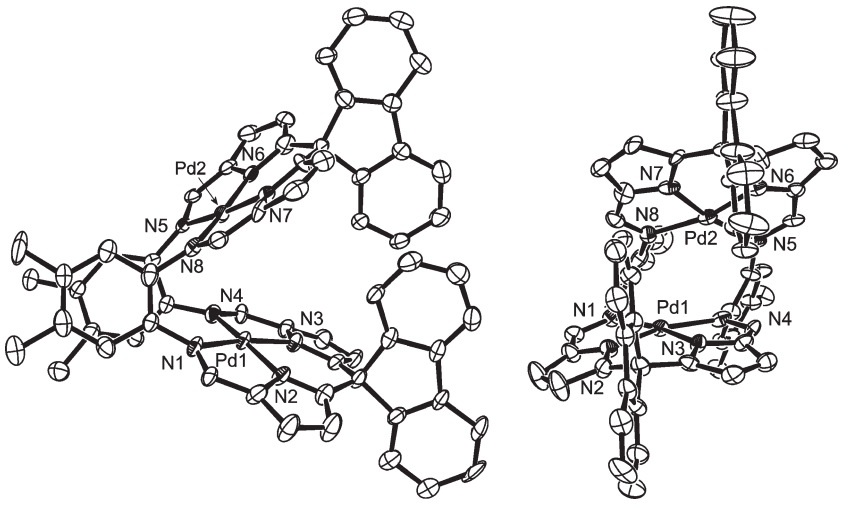

Figure 2. Solid state structure of $[Pd_2(L^1)](Et_2O)_{2.5}$ (left: side-on; right: face-on). For clarity, all hydrogen atoms and solvent of crystallization are omitted (displacement ellipsoids are drawn at 50% probability).

Table 3. Comparison of Geometric Parameters Derived from the X-ray Crystal Structures of a Series of Pacman Complexes of Schiff-Base Calixpyrrole Ligands

compound	M···M [Å]	twist [deg]	bite [deg]	ref
$[Pd_2(L^1)]$	3.72	27.8	56.4	this work
$[Pd_2(L^{Me8})]$	4.11/4.12[a]	11.1	62.1	17
$[Pd_2(L^{Ph4Me4})]$	3.94	28.5	59.7	17
$[Co_2(L^1)]$	3.64/3.64[a]	34.2	54.7	this work
$[Co_2(exo\text{-py})_2(L^1)]$	4.12	25.9	62.3	this work
$[Co_2(L^{Me4})]$	4.08/4.12[a]	31.3	62.6	8
$[Co_2(endo\text{-py})(exo\text{-py})(L^{Me4})]$	4.30/4.33[a]	2.9	64.8	7

[a] Two molecules in the asymmetric unit.

these structural parameters, for example, as seen in the series of complexes $[Cu_2(L)]$, they remain useful as a way of gaining some comparative insight into a series of interrelated compounds.[17] As a result of avoiding a steric clash between the *endo*-substituents both aryl-*meso*-substituted complexes display more twisted structures than the Me-substituted complex and results in shorter Pd···Pd separations and a decrease in the bite angle. In $[Pd_2(L^1)]$, it is clear that a π-stacking interaction between the *endo*-fluorenyl-substituents occurs (shortest interatomic separation 3.46 Å) and that these substituents are locked into a more sterically congested conformation, which contrasts to that seen with *meso*-Ph substituents that can undergo free rotation about the aryl-*meso*-C bond. To evaluate further the structural effects of the *meso*-fluorenyl substituents in these binuclear Pacman complexes, the cobalt complex $[Co_2(L^1)]$ and its bis(pyridine) adduct $[Co_2(py)_2(L^1)]$ were synthesized.

Synthesis and structure of $[Co_2(L^1)]$ and $[Co_2(py)_2(L^1)]$. The transamination reaction between H_4L^1 and $[Co(THF)\{N(SiMe_3)_2\}_2]$ in THF was carried out and generated the dark red, air-sensitive dicobalt complex $[Co_2(L^1)]$ in good yield (Scheme 1). The paramagnetic ^{1}H NMR spectrum of $[Co_2(L^1)]$ displayed 13 resonances between 74 and −51 ppm that support the adoption of a cleft-like structure in solution, and the room temperature magnetic moment of 3.24 μ_B by Evans' method is appropriate for an $S = 1$ spin ground state ($\mu_{calc} = 2.83\ \mu_B$). Metal coordination is corroborated further by a shift in the C=N stretch from 1616 cm^{-1} in H_4L^1 to 1551 cm^{-1} in $[Co_2(L^1)]$. The X-band EPR spectrum of $[Co_2(exo\text{-py})_2(L^1)]$ in frozen $CHCl_3$ consisted of a single, broad feature centered at $g = 2.217$. Dark-red crystals of $[Co_2(L^1)]$ were grown by hexane diffusion into toluene, and furthermore, addition of pyridine to the same crystallization solvent mixture generated dark red prisms of the bis(pyridine) adduct $[Co_2(exo\text{-py})_2(L^1)]$ that were suitable for X-ray crystallography; the solid state structures of $[Co_2(L^1)]$ and $[Co_2(exo\text{-py})_2(L^1)]$ were determined (Figure 3), and crystal data are shown in Table 1 with selected bond lengths and angles in Table 2.

In a manner similar to $[Pd_2(L^1)]$, the Co(II) cations in $[Co_2(L^1)]$ are coordinated in a square planar geometry by the two N_4-donor compartments (sum of the angles: Co1 359.7°; Co2 359.5°), and in an overall Pacman geometry. The lateral twist of the two donor compartments allows the two fluorenyl-substituents to interact to form a face-to-face π-stack (interplanar separation 3.77 Å) which results in a significantly shorter Co···Co separation and bite angle than in the *meso*-methyl-substituted analogue $[Co_2(L^{Me4})]$ (see Table 3). All other bond distances and angles are similar to those seen in previously reported examples.[7,8] The addition of pyridine to form the bis(pyridine) adduct $[Co_2(py)_2(L^1)]$ has a significant effect on the gross structure. While a Pacman geometry is still observed, the macrocycle is less twisted than in $[Co_2(L^1)]$ and results in a larger bite angle and an increase in the Co···Co separation. Surprisingly, both pyridine molecules are coordinated exogenously to the cleft, which suggests that this bimetallic microenvironment is spatially constrained, even though the mouth of the cleft has opened slightly on *exo*-pyridine complexation. Furthermore, the *exo*-fluorenyl groups interact with the pyridines in an edge-to-face π-stacking manner (C(H)···pyridine centroid 3.63 Å), with the pyridines arranged orthogonal to the fluorenyl-substituents. This structure contrasts to that of the *meso*-methyl-substituted analogue $[Co_2(endo\text{-py})(exo\text{-py})(L^{Me4})]$ in which one of the pyridine molecules binds to a Co(II) cation within the cleft, a mode that is stabilized by π-stacking interactions with the opposing pyrrole-imine compartment and also by a hydrogen-bonding interaction between the *meso*-methyl group and the orthogonal pyridine π-cloud.[7] The presence of this *endo*-pyridine also results in a significant decrease in the molecular twist angle, from 31.3° in $[Co_2(L^{Me4})]$,[8] to 2.9° in $[Co_2(endo\text{-py})(exo\text{-py})(L^{Me4})]$.[7] As such, it is clear that the presence of the fluorenyl-*meso*-substituent in H_4L^1 has a significant effect on the structural parameters of its complexes, resulting in compounds that retain a lateral twist and a more spatially constrained bimetallic cleft environment.

Synthesis and Structure of $[Pd_2(L^2)]$. The most straightforward route to the binuclear palladium complex of $[Pd_2(L^2)]$ was to form the potassium salt $[K_4(L^2)]$ in situ and to carry out a salt elimination reaction with $[PdCl_2(PhCN)_2]$ (Scheme 1). Alternatively, $[K_4(L^2)]$ could be isolated as the THF adduct $[K_4(THF)_{2.65}(L^2)]$, as demonstrated by elemental analysis and NMR data, and reacted separately with the Pd salt. The ^{1}H NMR spectrum of $[K_4(L^2)]$ shows very broad signals that can be assigned in general but are difficult to interpret. As such, the number of THF molecules per macrocycle was determined by quenching the potassium salt with wet d_5-pyridine which resulted in the recovery of H_4L^2 and 2.65 molecules of free THF by integration.

The reaction between $[Pd_2Cl_2(PhCN)_2]$ and $[K_4(L^2)]$ prepared in situ in THF in the dark formed, after 20 days, the binuclear complex $[Pd_2(L^2)]$ which crystallized from THF as a poorly soluble yellow solid in low yield; reactions for shorter time periods gave lower yields of the desired product. The ^{1}H NMR spectrum of $[Pd_2(L^2)]$ shows two sets of ethyl-*meso*-substituent resonances at 2.15/1.89 (CH_2) and 0.51/0.27 (CH_3) ppm that are characteristic of two non-equivalent ethyl groups and suggests that a cofacial ligand geometry has been adopted in solution. This feature is corroborated in the $^{13}C\{^1H\}$ NMR spectrum which displays ethyl group resonances at 40.0/36.6 (CH_2) and 11.2/10.4 (CH_3) ppm; the quaternary *meso*-carbon could not be located in the ^{13}C NMR spectrum because of the poor solubility of the compound. No N−H peak ($\upsilon = 3250$ cm^{-1} in H_4L^2) was observed in the IR spectrum of $[Pd_2(L^2)]$, and a shift

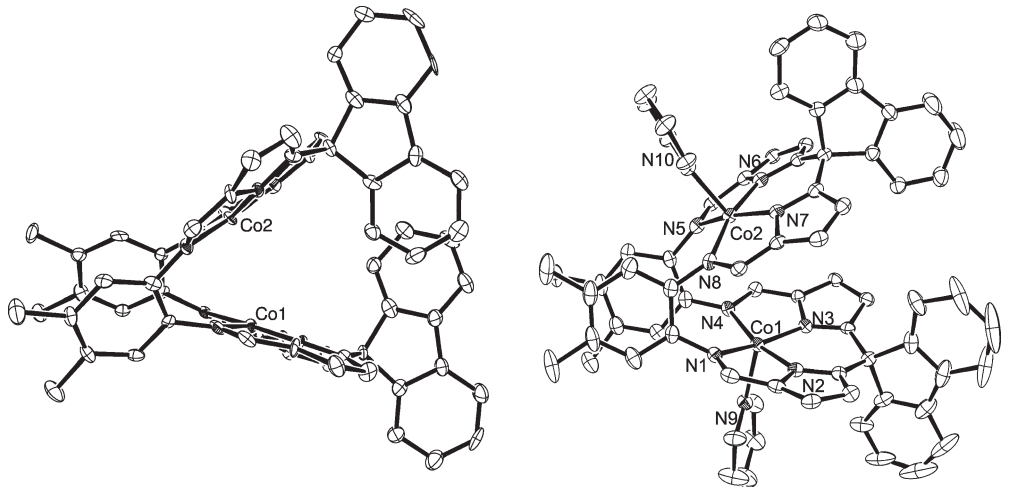

Figure 3. Solid state structures of $[Co_2(L^1)](PhMe)_2$ and $[Co_2(exo\text{-}py)_2(L^1)](PhMe)_{1.125}$. For clarity, all hydrogen atoms and toluene solvent of crystallization are omitted (displacement ellipsoids are drawn at 50% probability for $[Co_2(L^1)]$ and 25% probability for $[Co_2(exo\text{-}py)_2(L^1)]$).

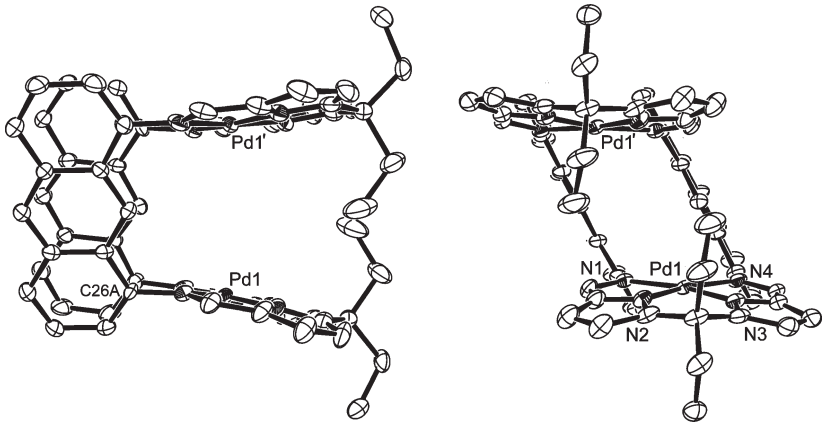

Figure 4. Solid state structure of $[Pd_2(L^2)](NEt_3)(CDCl_3)$ (Left: side-on view; right: face on view). For clarity, all hydrogen atoms and solvents of crystallization are omitted (displacement ellipsoids are drawn at 50% probability). The two palladium atoms Pd1 and Pd1′ are related by the symmetry operation $-x, y, 1/2 - z$.

in the C═N stretch to lower energies (from 1613 in H_4L^2 to 1570 cm^{-1}) supports the coordination of the metal by the macrocycle. The electrospray mass spectrum of $[Pd_2(L^2)]$ showed a molecular ion $[Pd_2(L^2)]^+$ at m/z 1070 and its sodium adduct $Na[Pd_2(L^2)]^+$ at m/z 1093 with the expected isotopic pattern, and elemental analysis further supported the proposed molecular formula. As an alternative synthetic procedure, $[Pd_2(L^2)]$ can also be accessed by the reaction between H_4L^2 and $[PdCl_2(PhCN)_2]$ in the presence of triethylamine, although yields from this route were generally lower and the complex more difficult to isolate. However, the ^1H NMR spectrum of the product from this route is identical to that described above, and yellow crystals of the binuclear palladium complex $[Pd_2(L^2)].NEt_3.CDCl_3$ were grown from a $CDCl_3$ solution. The X-ray crystal structure was determined, and the solid state structure is shown in Figure 4 with crystal data in Table 1 and selected bond lengths and angles detailed in Table 2.

As with $[Pd_2(L^1)]$, each N_4-donor compartment offers a *pseudo*-square-planar environment to the metal (sum of angles at Pd1 359.4°), and the palladium is located 0.122 Å out of the N_4 mean plane. In contrast however, the presence of the anthracenyl groups between the two metal-compartments in $[Pd_2(L^2)]$ has resulted in the formation of a double-pillared cofacial complex in which the two metal coordination planes are almost planar and show a slight divergence away from coplanarity (interplanar angle 15.3°); this slight deviation from coplanarity is likely attributable to a steric clash between the ethyl *meso*-substituents. The two anthracenyl backbones π-stack in a face-to-face manner (interatomic separation 3.43 Å) and are coplanar (interplanar angle 7.6°). Overall, the complex adopts a lateral twist of 29.4°, again due likely to sterically hindered interactions between the ethyl *meso*-substituents.

The structural parameters for $[Pd_2(L^2)]$ can be compared to related cofacial diporphyrin and corrole systems. Indeed, this ligand with its anthracenyl backbone proffers a geometric arrangement very similar to DPA (diporphyrinanthracene) and DCA (dicorroleanthracene),[24] and $[Pd_2(L^2)]$ can be viewed as a double-pillared analogue

(24) Ojaimi, M. E.; Gros, C. P.; Barbe, J.-M. *Eur. J. Org. Chem.* **2008**, *2008*, 1181.

Table 4. Comparison between the X-ray Structural Data of the Anthracenyl-Based Cofacial Diporphyrin and Dicorrole Complexes, and $[Pd_2(L^2)]$

compound	M···M [Å]	twist [deg]	interplanar angle[a]	ref.
[Pd2(L2)]	5.38	29.4	15.3	this work
[Co2(DPA)]	4.53	36.6	3.0	25
[Ni2(DPA)]	4.57	31.7	3.1	28
H4(DPA)	4.52[b]	22.1	−10.2	25
[Cu2(DCA)]	6.35[c]	19.9	18.9	29
[Ni2(DCA)]	4.68	22.4	9.4	30

[a] Angle between the best mean planes of the N_4-donor compartments. [b] Distance between the centroids of the two N_4-binding sites. [c] A molecule of PhMe is sandwiched within the bimetallic cleft.

of the series of well-known single-pillared complexes $[M_2(DPA)]$.[3,10,25,26] As the solid state structures of $[Pd_2(DPA)]$ and $[Pd_2(DCA)]$ are, to the best of our knowledge, unknown, the structurally characterized cofacial diporphyrin H_4DPA and its metal complexes $[Co_2(DPA)]$ and $[Ni_2(DPA)]$ are used for comparison (Table 4), along with the related dicorrole complexes $[Cu_2(DCA)]$ and $[Ni_2(DCA)]$. While the twist angle for $[Pd_2(L^2)]$ is similar to those seen in the structures of $H_4(DPA)$, $[Co_2(DPA)]$, and $[Ni_2(DPA)]$, the interplanar angle for $[Pd_2(L^2)]$ is larger than the diporphyrin analogues which suggests that the mouth of the cleft can expand vertically. This results in a Pd···Pd separation of 5.38 Å which is appreciably longer (by ca. 1.3 Å) than those seen in the 1,2-aryl-hinged complexes $[Pd_2(L^1)]$, $[Pd_2(L^{Me8})]$, and $[Pd_2(L^{Ph4Me4})]$ and similar to those observed for the related anthracenyl porphyrinic complexes (Table 4). Of the various binuclear DPA and DCA compounds that have been characterized structurally, the M···M separations (range: DPA 3.49 to 6.17; DCA 4.68 to 7.46 Å)[27] show that these ligands allow considerable vertical flexibility. In particular, the presence of endogenous solvent or ligands (e.g., MeOH) causes vertical expansion while single-atom bridging ligands (e.g., O or OH) promote closer interaction of the metallo-porphyrinic compartments. In our case, it is anticipated that the combination of the longer M···M separations and the presence of the very rigid double-anthracenyl pillars in $[M_2(L^2)]$ complexes will limit the stability of single-atom bridged complexes and so favor diatom binding.

Conclusions

We have shown that both the *meso*-fluorenyl-substituted and the anthracenyl-based Schiff-base calixpyrroles H_4L^1 and H_4L^2 can be prepared and that complexes of these macrocycles exhibit properties intrinsic to their design. The metal−metal separations in complexes derived from the *meso*-fluorenyl-substituted ligand H_4L^1 are comparable to, or larger than those found in complexes of the less bulky analogues because of an increased lateral twist, and, furthermore, the sterically hindering fluorenyl substituent prevents coordinating solvent from accessing the bimetallic cavity in the pyridine adduct $[Co_2(exo\text{-}py)_2(L^1)]$; presumably, this aspect will be important in preventing the formation of overly stable single-atom bridged complexes. As for the anthracenyl-based ligand H_4L^2, the metal−metal separation in $[Pd_2(L^2)]$ is increased significantly compared to the analogues derived from 1,2-diaminobenzene; as such, the metals should be sufficiently distant to favor the formation of diatom-bridged complexes. Significantly, the two N_4-donor compartments adopt a cofacial conformation in the solid state as a result of the π-stacked double-pillared arrangement of the anthracenyl hinges. We are currently investigating the formation of transition metal and f-element complexes of these new ligands and the effect that these designs have on their structural and catalytic chemistry.

Acknowledgment. We thank the Universities of Edinburgh and St. Andrews, the Sharif University of Technology, and the British Council of Iran for funding, and Dr's Manuel Volpe and Christopher D. Carmichael for their help with the X-ray crystallography.

(25) Bolze, F.; Drouin, M.; Harvey, P. D.; Gros, C. P.; Espinosa, E.; Guilard, R. *J. Porphyrins Phthalocyanines* **2003**, *7*, 474.

(26) Chang, C. K.; Liu, H. Y.; Abdalmuhdi, I. *J. Am. Chem. Soc.* **1984**, *106*, 2725. Collman, J. P.; Chng, L. L.; Tyvoll, D. A. *Inorg. Chem.* **1995**, *34*, 1311. Collman, J. P.; Fish, H. T.; Wagenknecht, P. S.; Tyvoll, D. A.; Chng, L.-L.; Eberspacher, T. A.; Brauman, J. I.; Bacon, J. W.; Pignolet, L. H. *Inorg. Chem.* **1996**, *35*, 6746. Collman, J. P.; Kim, K.; Leidner, C. R. *Inorg. Chem.* **1987**, *26*, 1152. Fujihara, T.; Tsuge, K.; Sasaki, Y.; Kaminaga, Y.; Imamura, T. *Inorg. Chem.* **2002**, *41*, 1170. Guilard, R.; Brandes, S.; Tabard, A.; Bouhmaida, N.; Lecomte, C.; Richard, P.; Latour, J.-M. *J. Am. Chem. Soc.* **1994**, *116*, 10202. Guilard, R.; Brandes, S.; Tardieux, C.; Tabard, A.; L'Her, M.; Miry, C.; Gouerec, P.; Knop, Y.; Collman, J. P. *J. Am. Chem. Soc.* **1995**, *117*, 11721. Guilard, R.; Lopez, M. A.; Tabard, A.; Richard, P.; Lecomte, C.; Brandes, S.; Hutchison, J. E.; Collman, J. P. *J. Am. Chem. Soc.* **1992**, *114*, 9877. Le Mest, Y.; Inisan, C.; Laouenan, A.; L'Her, M.; Talarmin, J.; El Khalifa, M.; Saillard, J.-Y. *J. Am. Chem. Soc.* **1997**, *119*, 6095. Liu, H. Y.; Abdalmuhdi, I.; Chang, C. K.; Anson, F. C. *J. Phys. Chem.* **1985**, *89*, 665. Naruta, Y.; Sasayama, M.; Ichihara, K. *J. Mol. Catal. A: Chem.* **1997**, *117*, 115. Ni, C. L.; Abdalmuhdi, I.; Chang, C. K.; Anson, F. C. *J. Phys. Chem.* **1987**, *91*, 1158. Osuka, A.; Maruyama, K.; Yamazaki, I.; Tamai, N. *Chem. Phys. Lett.* **1990**, *165*, 392. Pognon, G.; Wytko, J. A.; Harvey, P. D.; Weiss, J. *Chem.—Eur. J.* **2009**, *15*, 524. Proniewicz, L. M.; Odo, J.; Goral, J.; Chang, C. K.; Nakamoto, K. *J. Am. Chem. Soc.* **1989**, *111*, 2105. Sasayama, M.-a.; Naruta, Y. *Chem. Lett.* **1995**, 63. Yoshinori, S.; Sawada, N.; Tadokoro, M. *Chem. Lett.* **1994**, 1713.

(27) Fletcher, D. A.; McMeeking, R. F.; Parkin, D. *J. Chem. Inf. Comput. Sci.* **1996**, *36*, 746.

(28) Fillers, J. P.; Ravichandran, K. G.; Abdalmuhdi, I.; Tulinsky, A.; Chang, C. K. *J. Am. Chem. Soc.* **1986**, *108*, 417.

(29) Guilard, R.; Gros, C. P.; Barbe, J.-M.; Espinosa, E.; Jerome, F.; Tabard, A.; Latour, J.-M.; Shao, J.; Ou, Z.; Kadish, K. M. *Inorg. Chem.* **2004**, *43*, 7441.

(30) Jérome, F.; Barbe, J.-M.; Gros, C. P.; Guilard, R.; Fischer, J.; Weiss, R. *New J. Chem.* **2001**, *25*, 93.